Molecular Catalysis xxx (xxxx) xxx–xxx

Contents lists available at ScienceDirect

Molecular Catalysis

journal homepage: www.elsevier.com/locate/mcat

Synthesis, characterization and catalytic properties of cobalt oxide recovered from spent lithium-ion batteries

Carla G. Marcoccia[a], Miguel A. Peluso[a,b,*], Jorge E. Sambeth[a]

[a] CINDECA (CONICET-UNLP), 47 street, 257, La Plata, Argentina
[b] PlaPiMu-LaSeiSic (CICPBA-UNLP), Manuel B. Gonnet, Argentina

ARTICLE INFO

Keywords:
LIBs
Recycling
Co_3O_4
VOCs
Hydrometallurgy

ABSTRACT

Cobalt oxide was synthesized after a biohydrometallurgical process to recycle lithium-ion batteries (LIBs) from laptops. After separating the components of the spent LIBs, the cathodic material was leached with a bio-generated sulfuric acid at room temperature. Using 5% v/v H_2O_2 at 2 h, 60% Co was solubilized. After three successive lixiviation steps, 95% cobalt was solubilized. A cobalt oxide (CoO_x-R) was obtained by precipitation with $H_2C_2O_4$ and calcination at 500 °C, and was compared to both a cobalt oxide synthesized in the same way but using a commercial cobalt salt (CoO_x) and the cathodic material before leaching (LiCo). The characterization by XRD, FTIR, XPS and TPR demonstrated the presence of Co_3O_4 in CoO_x and CoO_x-R and $LiCoO_2$ phase in LiCo sample. CoO_x and CoO_x-R are better catalysts for VOC oxidation than LiCo due to higher S_{BET} and the presence of the Co_3O_4. CoO_x has a lower temperature for ethanol total oxidation but CoO_x-R produces less acetaldehyde than CoO_x. On the other hand, in toluene oxidation CoO_x and CoO_x-R present a similar performance, with a complete conversion near 300 °C. Cobalt oxide obtained using spent LIBs batteries as raw materials could be used as catalysts for VOC removal.

1. Introduction

Rechargeable lithium-ion batteries (LIBs) are the preferred batteries used in portable electronic devices such as laptops, cellular phones and camcorders, due to their high energy density, long lifespan, and safe handling [1,2]. The high number of LIBs in use worldwide turns into a large amount of end-of-life LIBs to be collected and treated.

LIBs are made of a cathode material (lithium metal oxide) on an aluminum foil, anode (graphite) on a copper foil, polymer electrolyte, plastic separator foil, binder (PVDF), metal casing, plastics and electronic control unit. The most expensive part of the battery is the cathode material, which utilizes a lithiated metal oxide or lithiated metal phosphate as the active material.

Laptop batteries are usually made of 4, 6 or 9 individual cylindrical cells 18 mm in diameter and 65.0 mm in length. The International Electrotechnical Commission (IEC) designates these batteries as 18650 cells, taking into account the diameter and length in millimeters [3]. Different parts of a typical laptop battery are listed in Table S1.

The active cathode material includes lithium mixed oxides such as $LiCoO_2$, $LiMn_2O_4$ (spinel), $LiNi_{1-x-y}Mn_xCo_yO_2$ (NMC), $LiFePO_4$ (LFP) or $LiNi_{1-x-y}Co_xAl_yO_2$ (NCA) [4]. One of the most commonly used materials in LIBs is $LiCoO_2$ because of its high energy density, high operating voltage, and good electrochemical performance.

The recycling of cobalt provides not only an environmental but also an economic benefit, taking into account that Co is a relatively expensive rare and precious metal, and has environmental toxicity [5,6] According to the London Metal Exchange (LME), the cobalt price in August 2018 been USD 62.70/kg.

Additionally to the benefits of recycling cobalt, the Al foil recovered from spent LIBs has the potential use for the preparation of catalyst support or catalyst material itself. In a recent work, Osman et al. [7] synthesized a mesoporous γ-Al_2O_3 with better surface characteristics than commercial alumina, using aluminum waste foil as raw material.

The recycling of batteries for metal recovery involves pyrometallurgical, hydrometallurgical or biohydrometallurgical processes. The pyrometallurgical process has disadvantages such as the emission of toxic gases.

In hydrometallurgical processes, metals in the separated cathode material are typically leached using inorganic acids such as HNO_3, H_2SO_4 and HCl, with the addition of H_2O_2 as reducing agent [8–11]. In order to avoid the use of inorganic acids, more recently, a variety of organic acids including citric acid, DL-malic acid, ascorbic acid, L-aspartic acid and oxalate [10–13] were also used to leach metal from spent LIBs.

* Corresponding author.
E-mail address: apelu@quimica.unlp.edu.ar (M.A. Peluso).

https://doi.org/10.1016/j.mcat.2018.10.018
Received 12 April 2018; Received in revised form 23 September 2018; Accepted 23 October 2018

The biohydrometallurgical process has been gradually replacing hydrometallurgical ones due to its higher efficiency, lower costs, few industrial requirements, and the possibility of on-site treatment. On-site sulfuric acid production has multiple advantages, since it eliminates the manipulation of concentrated sulfuric acid, the pollution from its industrial production, and transport costs [14].

Co_3O_4 has been proven to be an effective catalyst for the combustion of CO and hydrocarbons [15–17], VOC [18] and Cl-VOC [19]. The activity of Co_3O_4 is related to its strong redox ability and high bulk oxygen mobility, and the facile formation of highly active oxygen (O^- or O^{2-}) species [20–22].

It is known that deposition of a metallic oxide on an inert support with high surface area, leads to a catalyst with better catalytic performance than the oxide as a bulk catalyst. The acidity of the support and the addition of an oxygen carrier to the support influence the redox behavior of the oxides species and as a consequence the activity of the catalysts.

The optimised catalyst composition is therefore achieved through a balance of an acid support for increased electrophilicity which promotes rapid oxidation and an oxygen carrier for assisting reduction [23,24].

In a previous paper, we used a biohydrometallurgical process to recover Mn from spent alkaline and Zn/C batteries [25]. In this work, the biohydrometallurgical process is utilized for the leaching of metals from spent Li-ion batteries in order to recover Co in the form of oxide. The recovered Co oxide was investigated in the catalytic complete oxidation of two different VOC, ethanol and toluene, and compared with a cobalt oxide synthesized using commercial cobalt salt and with the cathodic material before leaching.

2. Experimental

2.1. Battery pretreatment

Spent LIBs from laptops were used in this work. Laptop batteries were collected from CICPBA Campus in the City of La Plata, Argentina. The plastic casing that holds the 18650 cells was manually removed. The batteries were then processed so they could be recycled. First, the cells were completely discharged to avoid short-circuiting by immersion in an electrolyte solution (5% NaCl, w/v) for 24 h and then washed with deionized water and dried at 90 °C for 12 h. Subsequently, they were manually opened making a cross-sectional cut in the metallic cover. The steel cases were removed from the cells, and the interior material was separated into plastic, aluminum sheets containing the cathodes, and copper sheets containing the anodes. The cathodic active material in the form of powder was separated from aluminum sheets by heating them at 250–300 °C for 30 min, which facilitated the detachment of the powder. The recovered powder was ground by milling and sieved to obtain a mesh size of less than 200 μm.

2.2. Leaching to recover metals from the calcined material

Leaching experiments were carried out using biogenerated sulfuric acid, produced in an air-lift type bioreactor, filled with sulfur, where a strain of *Acidithiobacillus thiooxidans* (*AT*) bacteria was inoculated. Details of the air-lift reactor and acid-reducing media production were described in previous papers [26].

All leaching experiments were performed in a 500-mL three-neck round-bottom flask with a magnetic stirrer, a sensor-based temperature controller, and a reflux condenser that was fitted to the flask to avoid loss due to evaporation. In all experiments, 3 g of recovered cathodic powder and 100 mL of a biogenerated sulfuric acid of pH = 0.8 were added to the reactor (solid/liquid relation, *S/L*, equal to 30 g L^{-1}). The effect of time of leaching and the addition of 5% v/v H_2O_2 on the extent of dissolution of metals was studied. A constant stirring speed of 500 rpm was maintained during the leaching. In order to monitor the progress of leaching, samples were taken at different time intervals, filtered and analyzed for metal contents. After leaching, a colored solution and a residual black material were obtained. The solution and the residual powder were separated by vacuum filtration.

In order to recover the most possible amount of cobalt, the residue of the lixiviation was treated again with fresh acid-reducing media and 5% v/v H_2O_2 (*S/L* = 30 g L^{-1}, 2 h and room temperature). Five successive leaching steps were studied.

2.3. Catalyst preparation

A cobalt oxide was recovered from spent lithium batteries and compared with a cobalt oxide prepared from commercial salts and with the cathode material obtained from spent batteries without leaching.

Recovered cobalt oxide (CoO_x-R): After leaching, the pH of the solution was increased to 4 with NaOH addition. Then 100 mL of $H_2C_2O_4$ 0.100 M (anhydrous 99%) was added dropwise to 100 mL of the leachate liquor, in order to precipitate CoC_2O_4, and the suspension was stirred at 30 °C for 1 h. A pink product was obtained, which was filtered, washed with distilled water, and dried at 120 °C for 24 h. Finally, the solid was calcined in air at 500 °C for 2 h.

Synthetic cobalt oxide (CoO_x): 100 mL of $H_2C_2O_4$ 0.100 M (anhydrous 99%) was added dropwise to 100 mL of 0.100 M $Co(CH_3CO_2)_2$ solution following the same procedure described above.

LiCo: For comparison purposes, a part of the recovered cathodic material was calcined at 750 °C in air for 3 h in order to eliminate some carbon residues.

A diagram of the complete procedure to recover metals from spent LIBs is shown in Fig. 1.

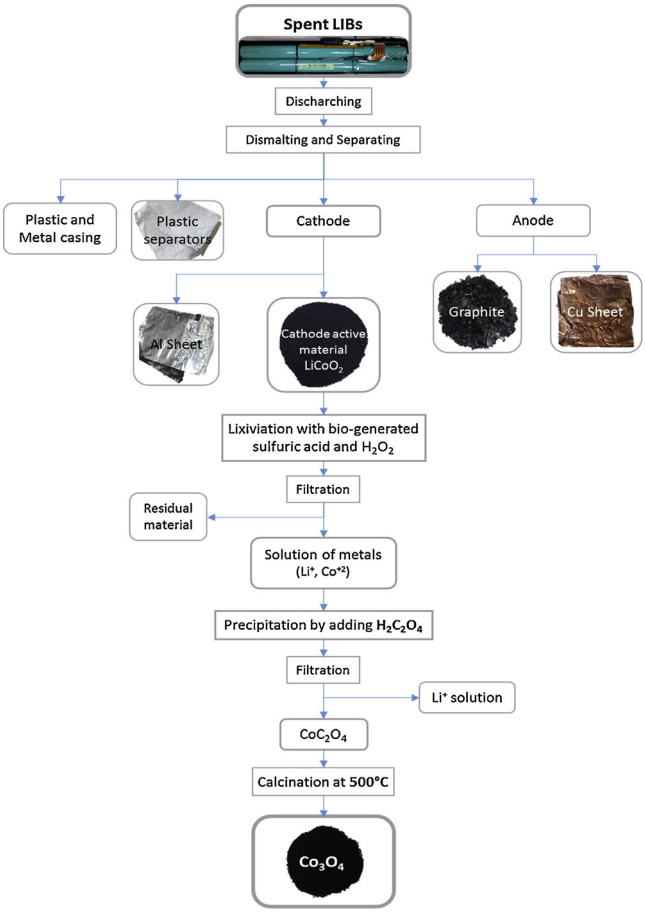

Fig. 1. Flow-sheet of the procedure to recover cobalt from spent LIBs.

2.4. Characterization

Lithium and cobalt concentration were measured in a Varian AA 240 spectrophotometer. Metal concentration in the cathode material was measured also by AA after digestion by HNO_3–HCl (1:3) method.

The X-ray diffraction (XRD) patterns were taken using a Philips PW1390 diffractometer. The diffraction patterns were recorded at room temperature from 15 to 80° of 2θ using Cu Kα (λ = 1.5406 Å) radiation at 0.02° min^{-1} scanning speed and a counting time of 2 s per step.

The scanning electron microscopy (SEM) and dispersive X-ray analysis (EDS) were performed in a Philips SEM 505 microscope.

Textural properties of the oxides were determined in a Micromeritics Accusorb 2100 D sorptometer by BET method.

X-ray photoelectron spectra (XPS) of the oxides were acquired using a multitechnique system, equipped with a hemispherical PHOIBOS 100 MCD, SPECS analyzer. X-rays were produced by a monochromatized aluminum anode (1486.6 eV) radiation (13 kV, 300 W). C 1 s = 284.6 eV was used as the internal reference. CasaXPS program (Casa Software Ltd., UK) was used for curve fitting.

FTIR spectroscopy studies were performed on a Bruker IFS66 infrared spectrometer at a spectral resolution of 4 cm^{-1} accumulating 200 scans.

Temperature programmed reduction (TPR) experiments were performed using a 5% H_2 in N_2 as reducing gas (22 cm^3 min^{-1}), with a heating rate of 10 °C min^{-1}. The amount of solid employed was 50 mg and temperature was increased from room temperature to 900 °C.

2.5. Catalytic activity

The catalytic activity of the samples was evaluated in a flow U-shape glass reactor at atmospheric pressure using 100 mg of catalyst. Total gas flow was 50 cm^3 min^{-1} (gas hourly space velocity of 18,000 h^{-1}) and a VOC concentration of 2% v/v in air. VOC conversion and conversion into acetaldehyde were analyzed by GC-FID (Thermo Finnigan Trace GC). Conversion into CO_2 was measured by an on-line CO_2 detector (Telaire CO_2 sensor). The conversion of VOC (X) and the conversion into CO_2 (X_{CO2}) and into acetaldehyde (X_{acetal}) were calculated as $X = 1- F_{VOC}/F_{VOC,in}$; $X_{CO2} = F_{CO2}/\nu F_{VOC,in}$ and $X_{acetal} = F_{acetal}/F_{ethanol,in}$, where F_{VOC} is the outlet molar flow rate of VOC (ethanol or toluene) at steady state, $F_{VOC,in}$ is the inlet molar flow rate of VOC, F_{CO2} is the outlet molar flow rate of CO_2 at steady state (ν is the number of carbon atoms in the VOC molecule), and F_{acetal} is the outlet molar flow rate of acetaldehyde at steady state. Carbon balance is near 100%.

3. Results and discussion

The composition of each individual 18650 cell used in this work is represented in Table S2. The cathode material represents 34 wt% of the individual cell, with a composition of 51.0 wt% Co and 3.3 wt% Li.

The X-ray diffraction patterns of the cathode material as well as the residue after three successive leaching steps are depicted in Fig. S1. The cathode material before leaching presents diffraction peaks corresponding to $LiCoO_2$ [27]. The residue also shows diffraction lines corresponding to $LiCoO_2$ but with much lower intensity than the started material.

Fig. S2 shows a SEM images and EDS analyses of the spent cathodic material and the residue after three successive leaching steps. The morphology of the spent cathodic material (Fig.S2a) was identified as irregular and agglomerated with particle diameters of 6–20 μm, in accordance with other authors [6,28]. SEM image of the residue (Fig.S2b) shows a spread corrosion of the particles. The EDS analyses show that the Co intensity is diminished and carbon intensity is increased after three successive leaching steps. Additional, the presence of S was identified in the residual solids, as a result of the sulfuric acid used in the leaching process.

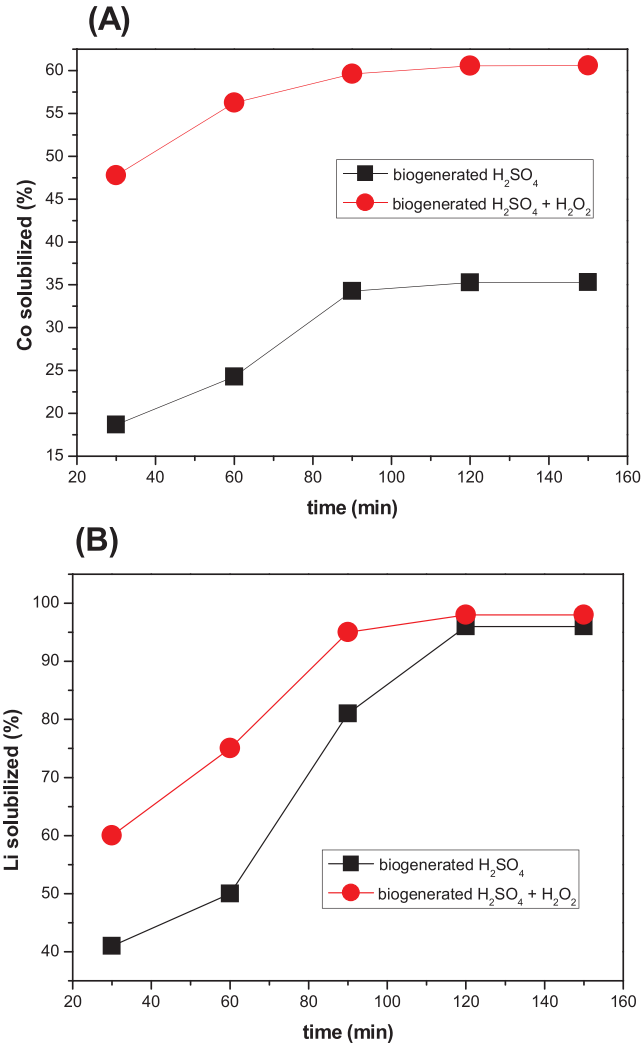

Fig. 2. Extraction efficiency of metals as a function of time: (A) Co and (B) Li, using bio-generated sulfuric acid with and without H_2O_2 (S/L = 30 g L^{-1}, 30 °C).

3.1. Evaluation of leaching conditions

In the $LiCoO_2$ material, the valence of Li and Co is 1+ and 3+, respectively [29]. The dissolution of the cathodic material involves the reduction of Co^{3+} to Co^{2+} [30]. Therefore, to improve the leaching efficiency, a reducing agent is required. If only sulfuric acid is used, metals may be dissolved according to the following equation:

$$4LiCoO_2 + 6H_2SO_4 \rightarrow 2Li_2SO_4 + 4CoSO_4 + O_2 + 6H_2O \quad (1)$$

where the oxygen of the mixed oxide is oxidized to O_2 gas, thus leading to the low efficiency of Co leaching. As described in a previous paper [26], the biogenerated sulfuric acid contains also polythionates species, which can act as reducing agents. So, with the use of biogenerated sulfuric acid, the dissolution of $LiCoO_2$ could proceed according to the following equation:

$$2LiCoO_2 + S_n(SO_3)_2^{2-} \rightarrow Li_2SO_4 + 2CoSO_4 \quad (2)$$

The effect of time on the leaching efficiencies using biogenerated sulfuric acid is shown in Fig. 2. Cobalt leaching efficiency increased from about 20% to 36% when the leaching time increased from 30 to 120 min. Cobalt extraction remained at the same values with more leaching time. Lithium leaching efficiency increased from 40% to almost 100% when the leaching time increased from 30 to 120 min. Even though the biogenerated sulfuric acid has reducing species, it is evident

that their concentration is not enough for an efficient leaching. The biogenerated sulfuric acid using in this work is equivalent to 0,10 M sulfuric acid solution plus 0,05 M polythionates [26]

In order to increment cobalt extraction efficiency, a reducing agent, H_2O_2, was added.

With the addition of H_2O_2 to the biogenerated sulfuric acid, the dissolution of $LiCoO_2$ could proceed according to the following equation:

$$2LiCoO_2 + 3H_2SO_4 + H_2O_2 \rightarrow Li_2SO_4 + 2CoSO_4 + O_2 + 4H_2O \quad (3)$$

These equations show that the addition of the reacting substances can facilitate the forward reaction resulting in an increase in cobalt extraction efficiency.

As was shown in Fig. 2, at 120 min, the dissolution efficiency of Co increased from 36% to 60% when H_2O_2 was added.

Fig. S3 shows the results of cobalt extraction after five successive leaching steps. Fig. S3 (A) represents the cobalt extraction efficiency in each leaching steps, whereas Fig. S3(B) shows the cumulative cobalt extraction efficiency. After three successive extractions with bio generated sulfuric acid and H_2O_2, the cobalt extraction reaches an efficiency of more than 95%. Additionally steps of lixiviation do not improve significantly the cobalt extraction. Tables S3 and S4 lists the costs of reactants and expected benefits of recycling LIBs, scale to 1 ton of batteries. It was considered the case using biogenerated sulfuric acid with H_2O_2 in one step. The cost of the biogenerated sulfuric acid was considered negligible.

The balance results in a profit margin of USD 4306. It is noted that we only consider the material balance. The labor, equipment and energy costs will be added in the future in the economic analysis.

3.2. Synthesis and characterization of cobalt oxides

After leaching, a cobalt oxide was prepared and compared with a cobalt oxide prepared in the same way but using a commercial cobalt salt as a Co^{2+} source. Additionally, the oxide recovered from spent LIBs and calcined at 750 °C was compared. The selected temperature was used in order to remove carbon from the cathodic material.

Table 1 lists the textural properties of the samples studied. The recycled cobalt oxide presents a specific surface area similar to that of the cobalt oxide synthesized using commercial salts. On the other hand, the calcined cathode material has a low surface area.

An XRD pattern of the recovered cobalt oxalate is shown in Fig. 3(A). The pink product obtained presents diffraction lines corresponding to $CoC_2O_4.2H_2O$. After calcination in air at 500 °C, a solid powder was obtained. The X-ray diffraction pattern depicted in Fig. 3 (B) shows that the recycled cobalt oxide presents the diffraction lines corresponding to Co_3O_4, (JCPDS: 42–1467) and no other peaks appear. The cobalt oxide prepared using commercial salts also exhibits diffraction lines associated with Co_3O_4. The cathode material after calcination (LiCo) presents the diffraction peaks corresponding to the well-crystallized $LiCoO_2$ single phase (Fig.3(C)) [27].

The morphology of the recovered cobalt oxide, as well as the oxalate precursor, was characterized by SEM, as shown in Fig. 4. The SEM images of recovered oxalate before and after decomposition are rather similar. The external shape of the oxalate particles (rod like) is kept [31]. Furthermore, the obtained CoO_x-R has some fiber-like particles with a size of about several hundreds of nanometers, in agreement with

Table 1
Textural properties of the samples.

Catalyst	S_{BET} ($m^2 g^{-1}$)	Vp ($cm^3 g^{-1}$)	Dp (A)
CoO_x R	14	0.08	202
CoO_x	16	0.12	194
$LiCoO_2$	0.8	0.14×10^{-3}	103

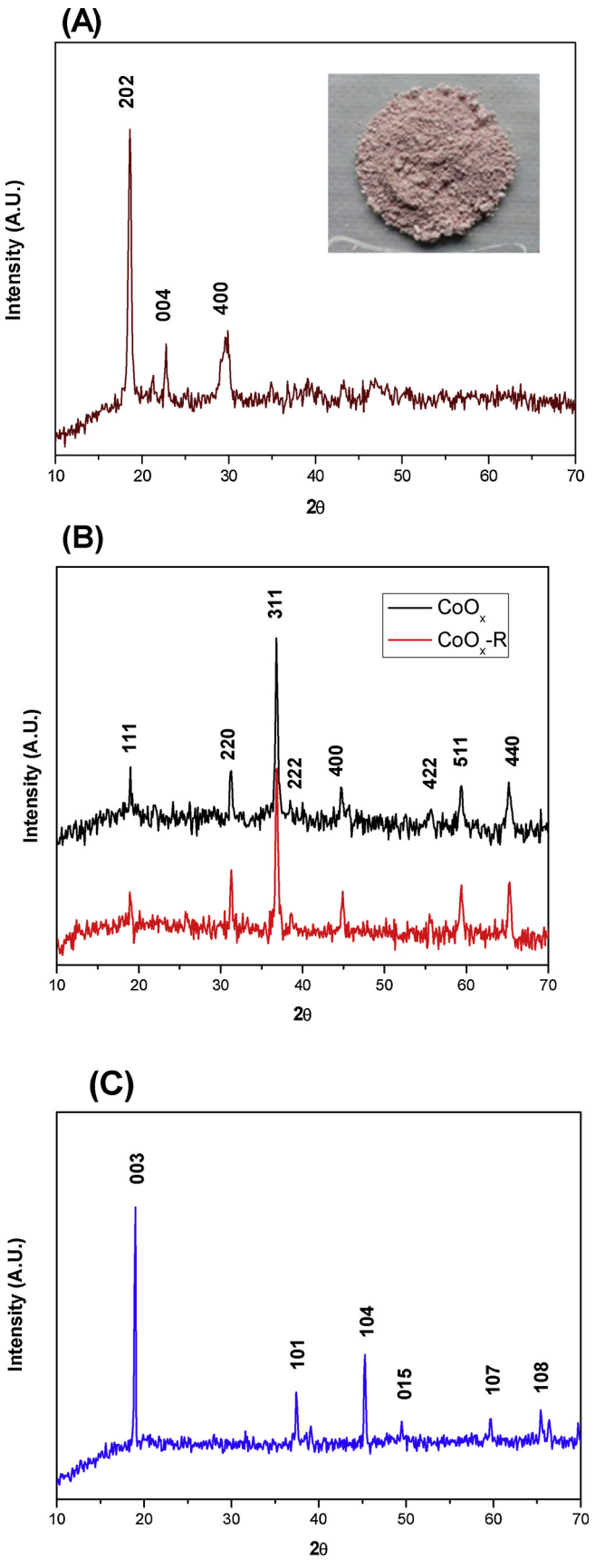

Fig. 3. X-ray diffraction patterns of the samples: (A) recovered $CoC_2O_4.2H_2O$ and (B) CoO_x and CoO_x-R samples and (C) LiCo sample.

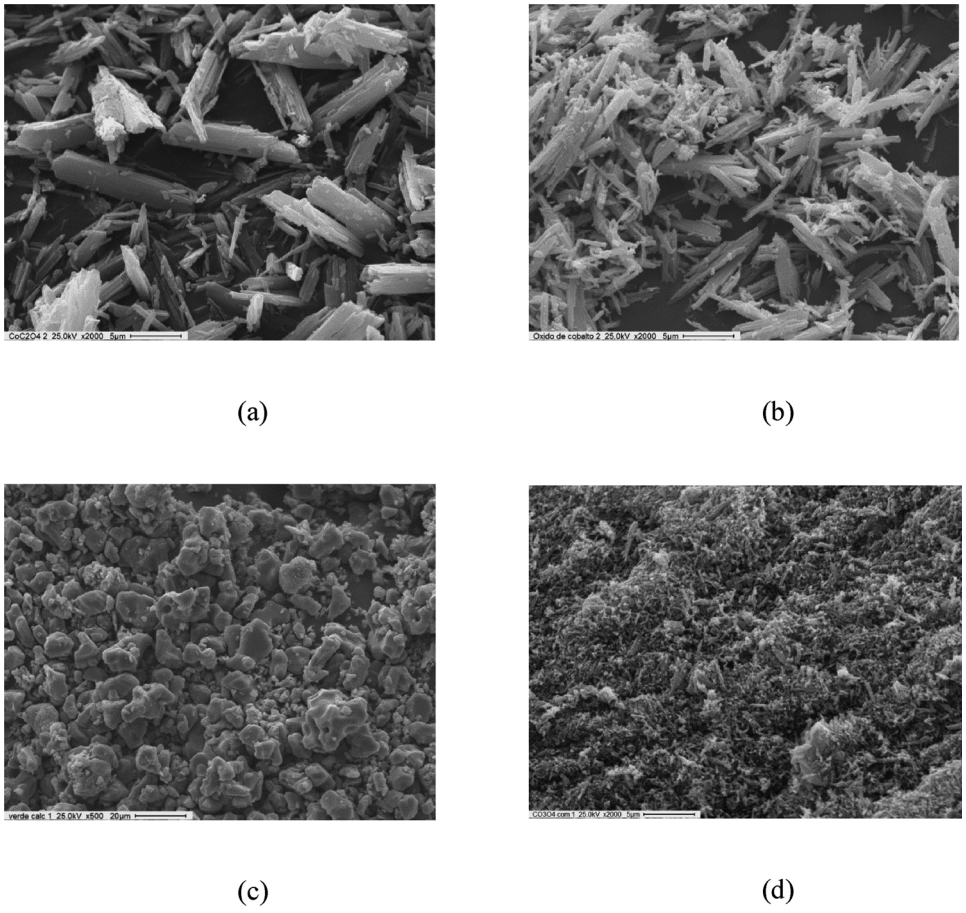

Fig. 4. SEM micrographs of cobalt oxides and precursors: (a) recovered $CoC_2O_4.2H_2O$; (b) CoO_x-R and (c) CoO_x.

Liu et al. [32]. The sample CoO_x presents particles of smaller size than the recovered cobalt oxide.

The FTIR spectra of samples are depicted in Fig. 5. In both oxides with Co_3O_4 structure, bands corresponding to Co-O stretching can be seen at nearly 560 and 600 cm^{-1}. The signal between 1000 and 1200 cm^{-1} in the CoO_x-R sample could be associated with SO_4^{2-} species coming from sulfuric acid. The spectrum of the LiCo sample is similar to that reported in the bibliography for $LiCoO_2$, characterized by a peak at 599 cm^{-1} and no organic compounds were detected [27].

Fig. 6 shows the Co 2*p* XPS spectra of the samples. The recycled cobalt oxide material presents two major peaks at binding energies of 794.8 and 779.8 eV, with spin-separation energy of 15.1 eV, corresponding to the Co $2p_{1/2}$ and Co $2p_{3/2}$ spin-orbit peaks of Co_3O_4. [33–37].

The CoO_x sample also shows the characteristic Co 2*p* doublet (Co $2p_{3/2}$ and Co $2p_{1/2}$) related to the spin-orbit splitting of 15.2 eV characteristic of Co_3O_4.

The LiCo sample shows Co 2*p* spectra of much lower intensity than the CoO_x-R and CoO_x oxides due to their lower Co content.

The corresponding O 1*s* spectra of the samples are depicted in Fig. 7. The CoO_x and CoO_x-R samples are characterized by a very intense band at around 529.5 eV (O_I), which can be assigned to lattice oxygen. A second well-resolved peak at around 531.2 eV (O_{II}) is related to surface oxygen, oxygen vacancies, as well as to hydroxyl/carbonate groups [38]. In general, O_{II} species are considered responsible for total oxidation reactions, and presents greater mobility than O_I species [39,40]. In the samples CoO_x and CoO_x-R, the O_{II}/O_I ratio was 1.17 and 0.87, respectively

The O 1*s* spectrum of LiCo shows a single peak at 530.6 eV, which is related to $Li_{1-x}CoO_2$ material [41].

TPR profiles of the samples are presented in Fig. 8. The peaks observed in the range of 200–450 °C were attributed to the successive reduction of Co_3O_4 to CoO and to the reduction of CoO to metallic cobalt (Co^o) [42,43]. The increase in temperature for the reduction of CoO_x-R sample might be due to the increase in crystallite sizes, which might require higher temperature for their reduction [44].

The band observed at 655 °C in the CoO_x-R sample could be due to the reduction of sulfate impurities [45]. In the case of LiCo sample, the reduction events are shifted to higher temperatures. $LiCoO_2$ is reduced to Co° (through Co^{2+} intermediate specie) and Li_2O [46].

3.3. Catalytic activity

The catalytic performance of the prepared samples was evaluated in the complete oxidation of ethanol and toluene.

Fig. 9 (A) shows the light-off curves for ethanol oxidation. CoO_x presents the lowest T_{50} and T_{90} (temperatures at 50% and 90% of ethanol conversion, respectively), followed by CoO_x-R and LiCo. The conversion to CO_2 (Fig. 9 (B)) shows the same tendency as ethanol conversion. The discrepancy between ethanol oxidation and CO_2 yield curves is the formation of acetaldehyde, a partial oxidation product of ethanol oxidation. The conversion to acetaldehyde (Fig. 9 (C)) reaches a maximum at approximately 250 °C with a yield of 0.15 for CoO_x catalyst. In the recovered oxide, CoO_x-R, the maximum of acetaldehyde appears at near 258 °C, slightly higher than the reference catalyst. Nevertheless, the acetaldehyde yield in CoO_x-R is much lower (0.05) than in CoO_x, representing a benefit in VOC oxidation reaction, taking into accounts that acetaldehyde is more harmful to human health and the environment than ethanol.

The selectivity to acetaldehyde is influenced by many various

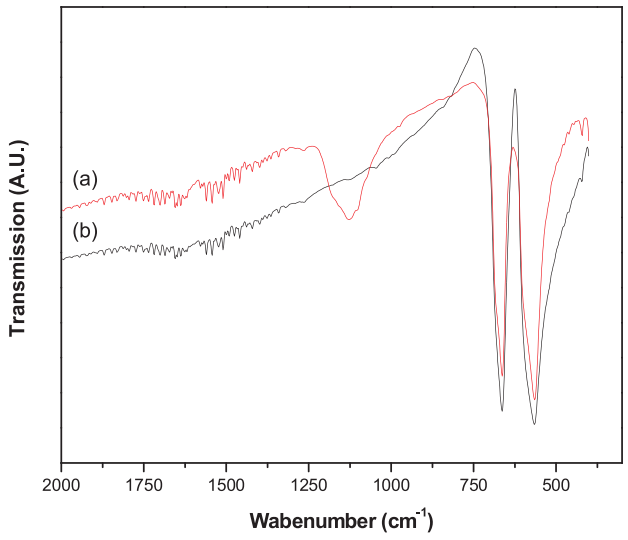

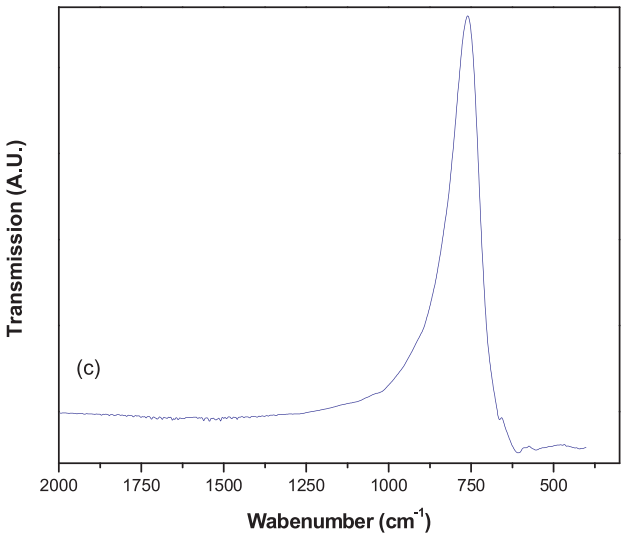

Fig. 5. FTIR spectra of the samples: (a) CoO_x-R, (b) CoO_x and (c) LiCo.

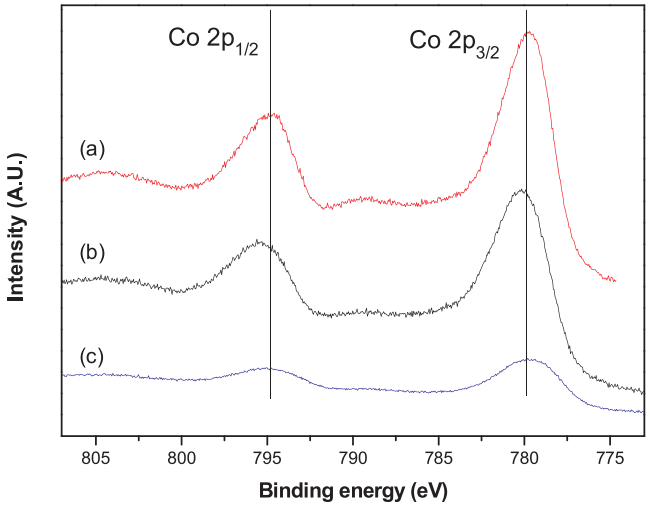

Fig. 6. Co 2*p* XPS spectra of the samples: (a) CoO_x-R, (b) CoO_x and (c) LiCo.

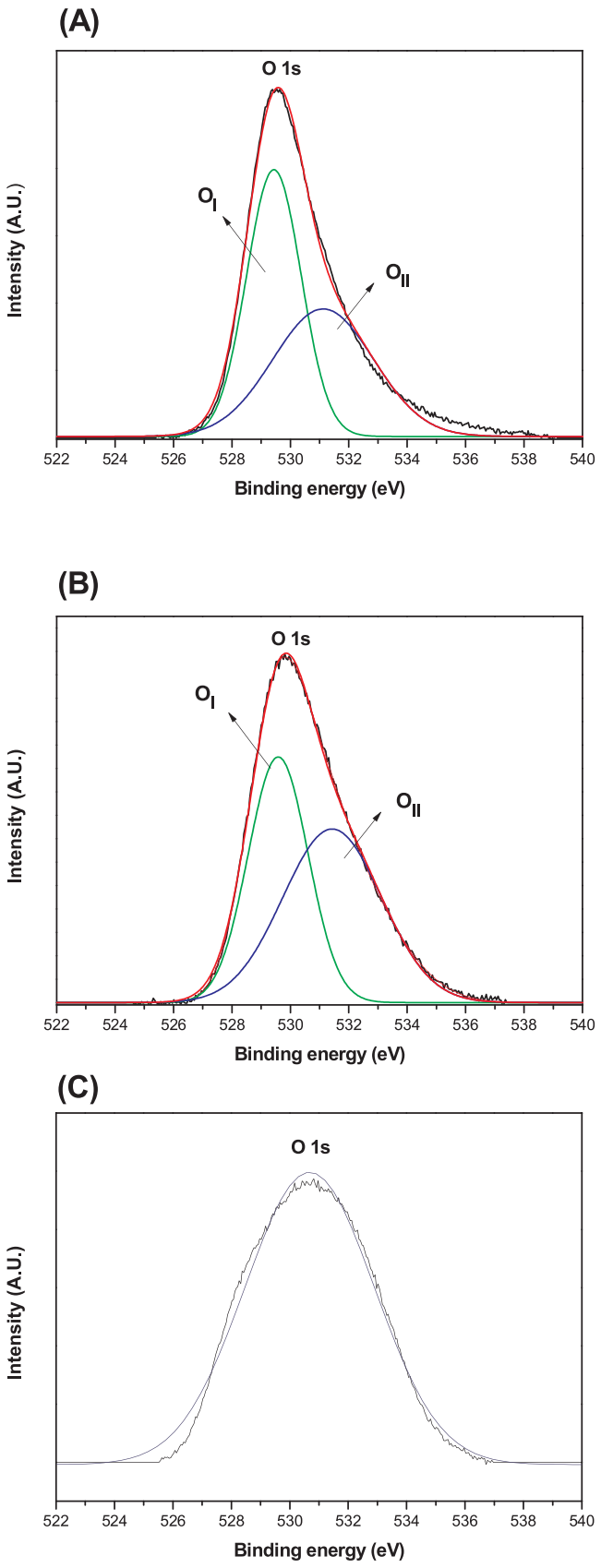

Fig. 7. O 1*s* XPS spectra of the samples. (A) CoO_x-R; (B) CoO_x and (C) LiCo.

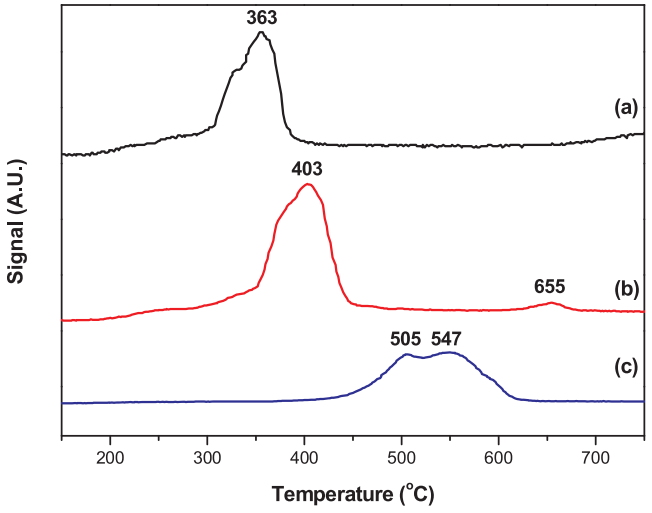

Fig. 8. TPR plots of the samples: (a) CoO_x, (b) CoO_x-R and (c) LiCo.

parameters. It is reported that oxidative dehydrogenation of ethanol to acetaldehyde is catalyzed by materials possessing strong base sites [47] and increased basicity of the catalysts increased catalyst reducibility [48]. On the other hand, the presence of SO_4^{2-} species could also be responsible for lower acetaldehyde yield over CoO_x-R [49].

Gallegos et al. [50] in their studies of ethanol oxidation on catalysts obtained from spent alkaline batteries also found that acetaldehyde yield was lower over recycled MnO_x than commercial MnO_x.

In the case of LiCo sample, the maximum of acetaldehyde appears at higher temperatures, 307 °C, and with a higher yield, 0.17.

The light-off curve of toluene oxidation is shown in Fig. 10. Conversely to ethanol oxidation, the only carbon containing product detected in toluene oxidation was CO_2 at all conversion levels, and $X_{CO2} = X_{tol.}$ CoO_x catalyst again presents the lowest T_{50} and T_{90}, although differences between the CoO_x-R catalyst is less pronounced.

As we have seen, the lowest specific surface area oxide (LiCo) has the lowest ethanol and toluene conversion. The surface are of both catalysts with Co_3O_4 structure are of the same order.

It is accepted that the catalytic activity of Co_3O_4 in VOC oxidation reactions is associated with its reduction ability [18,51,52]. In our work, a clear correlation between catalytic activity and redox properties was found. The lower the T_{50} and T_{90} in VOC oxidation, the lower the reduction temperature in TPR experiments.

Additionally, XPS results show that the concentration of O_{II} species is slightly higher in the catalyst with the high VOC conversion, CoO_x, than in CoO_x-R. This result is in agreement with Santos et al. [53] who have found a correlation between O_{II} species and VOC conversion.

VOC conversion on CoO_x-R is not much lower than in CoO_x, and, additionally, the production of incomplete oxidation products in CoO_x-R catalyst is low.

The evolution with long-time durability of ethanol and toluene combustion over CoO_x-R catalyst is shown in Fig. 11. During 60 h of reaction under dry conditions, the ethanol and toluene conversion is constant during the study, indicating the stability of the recycled cobalt oxide obtained.

Among different techniques to prepare cobalt oxide such as thermal decomposition, solid-state reaction, wet-chemical and sol–gel methods, De Rivas et al. [21] found that oxides synthesized by precipitation were the most active for VOC oxidation.

Precipitation is an easy way to synthesize catalysts and this is important considering an eventual scale-up of the whole process.

These features render cobalt catalysts prepared using spent LIBs as raw material suitable for reducing VOC emissions. Furthermore, the cost of the biological production of sulfuric acid is below the cost of a commercial one and can be reduced even more [26].

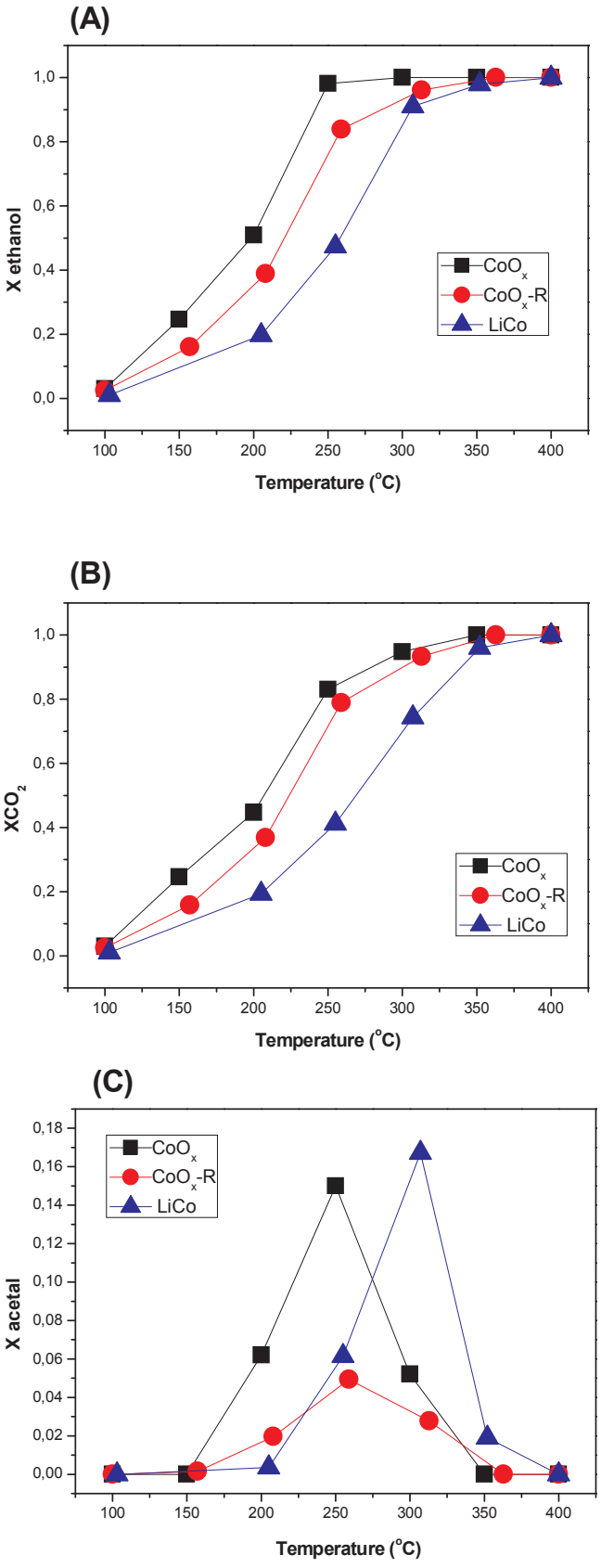

Fig. 9. Light-off curves of ethanol over the samples: (A) ethanol conversion, (B) conversion to CO_2 and (C) conversion to acetaldehyde.

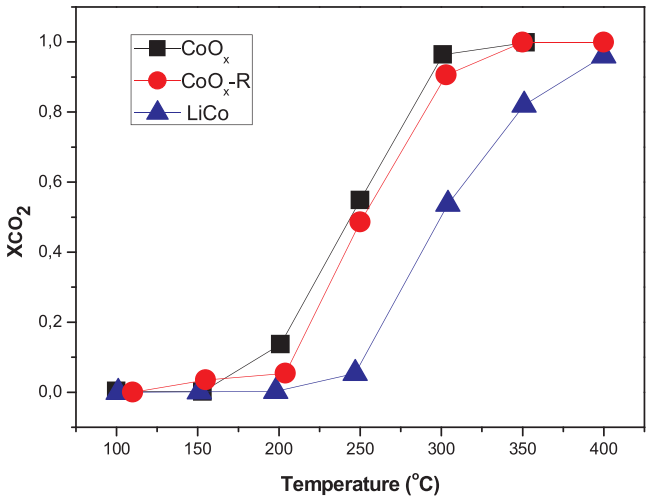

Fig. 10. Light-off curves of toluene over the catalyst.

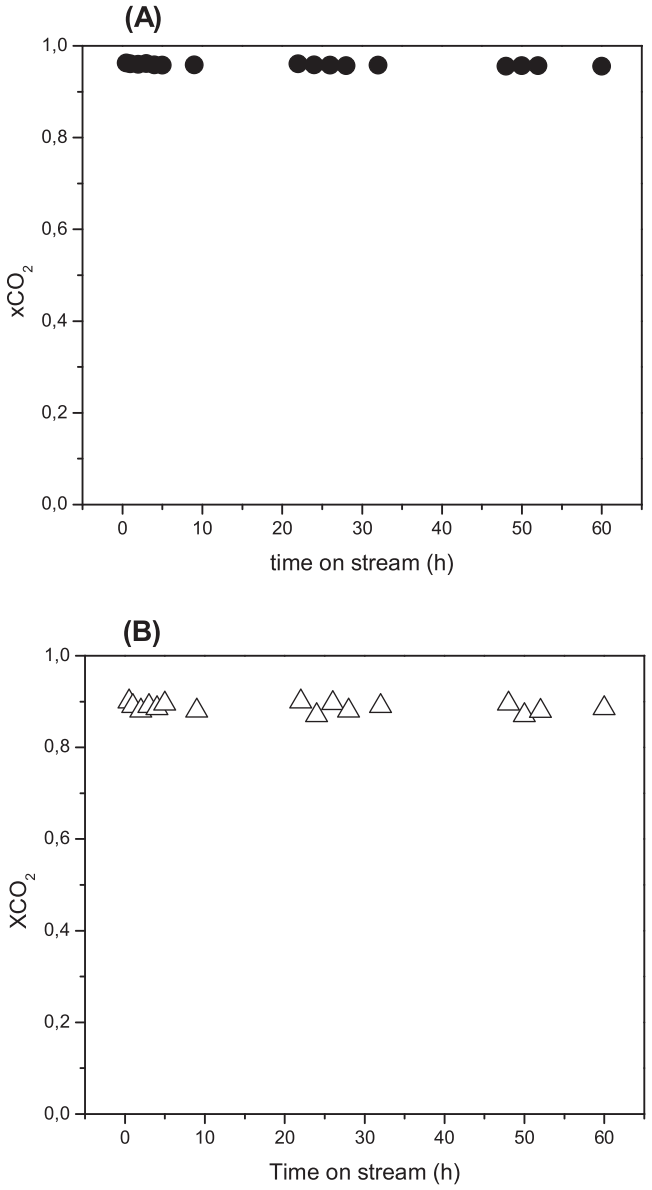

Fig. 11. Stability test: (A) ethanol and (B) toluene conversion as a function of reaction time.

4. Conclusions

A biogenerated sulfuric acid was used as leaching agent in order to develop an eco-friendly recycling route for spent Li-ion batteries containing $LiCoO_2$ as cathode active material. With three successive lixiviation steps, more than 95% of cobalt was solubilized at room temperature. Cobalt was recovered from the leaching solution by precipitation with $H_2C_2O_4$ and further calcination at 500 °C, and compared with both a cobalt oxide synthesized using a commercial cobalt salt and the cathode material after calcination. XRD, XPS and TPR analyses indicate that the recovered material (CoO_x-R) presents the Co_3O_4 phase.

The VOC conversion depends on the presence of the Co_3O_4 phase, the S_{BET}, the reducibility of the samples and the higher O_{II}/O_I ratio. Although ethanol conversion decreases in the order: CoO_x > CoO_x-R > LiCo, acetaldehyde production in CoO_x-R is lower than that of CoO_x. On the other hand, toluene conversion over CoO_x and CoO_x-R are rather similar. Additionally, CoO_x-R presents excellent stability during long-time run.

This work shows that spent lithium-ion batteries can be used as raw materials to prepare cobalt oxide, which can be used as efficient catalysts for the total oxidation of volatile organic compound emissions, using an eco-friendly recycling process.

Acknowledgements

The authors acknowledge the CONICET and UNLP (Argentina). We are thankful to Lic. P. Fetsis and Lic. M. Theiller. This work was supported by CONICET (PIP 942), CICPBA and ANPCyT (PICT 2012-2366) – Argentina.

Appendix A. Supplementary data

Supplementary material related to this article can be found, in the online version, at doi:https://doi.org/10.1016/j.mcat.2018.10.018.

References

[1] T. Zhang, Y. He, F. Wang, L. Ge, X. Zhu, H. Li, Chemical and process mineralogical characterizations of spent lithium-ion batteries: an approach by multi-analytical techniques, Waste Manag. 34 (2014) 1051–1058, https://doi.org/10.1016/j.wasman.2014.01.002.

[2] J. Lee, A. Urban, X. Li, D. Su, G. Hautier, G. Ceder, Unlocking the Potential of Cation-Disordered Oxides for Rechargeable Lithium Batteries, Science 343 (2014) 519–522.

[3] T. Reddy, Linden's Handbook of Batteries, 4th ed., (2011) New York.

[4] J. Xu, H.R. Thomas, R.W. Francis, K.R. Lum, J. Wang, B. Liang, A review of processes and technologies for the recycling of lithium-ion secondary batteries, J. Power Sources 177 (2008) 512–527, https://doi.org/10.1016/j.jpowsour.2007.11.074.

[5] G.P. Nayaka, K.V. Pai, J. Manjanna, S.J. Keny, Use of mild organic acid reagents to recover the Co and Li from spent Li-ion batteries, Waste Manag. 51 (2016) 234–238, https://doi.org/10.1016/j.wasman.2015.12.008.

[6] L. Li, J.B. Dunn, X.X. Zhang, L. Gaines, R.J. Chen, F. Wu, K. Amine, Recovery of metals from spent lithium-ion batteries with organic acids as leaching reagents and environmental assessment, J. Power Sour. 233 (2013) 180–189, https://doi.org/10.1016/j.jpowsour.2012.12.089.

[7] A.I. Osman, J.K. Abu-Dahrieh, M. McLaren, F. Laffir, P. Nockemann, D. Rooney, A facile green synthetic route for the preparation of highly active γ-Al_2O_3 from aluminum foil waste, Nat. Sci. Rep. 7 (2017) 3593, https://doi.org/10.1038/s41598-017-03839-x.

[8] C.K. Lee, K.I. Rhee, Reductive leaching of cathodic active materials from lithium ion battery wastes, Hydrometallurgy 68 (2003) 5–10, https://doi.org/10.1016/S0304-386X(02)00167-6.

[9] R.C. Wang, Y.C. Lin, S.H. Wu, A novel recovery process of metal values from the cathode active materials of the lithium-ion secondary batteries, Hydrometallurgy 99 (2009) 194–201, https://doi.org/10.1016/j.hydromet.2009.08.005.

[10] M.K. Jha, A. Kumari, A.K. Jha, V. Kumar, J. Hait, B.D. Pandey, Recovery of lithium and cobalt from waste lithium ion batteries of mobile phone, Waste Manag. 33 (2013) 1890–1897, https://doi.org/10.1016/j.wasman.2013.05.008.

[11] J. Kang, G. Senanayake, J. Sohn, S.M. Shin, Recovery of cobalt sulfate from spent lithium ion batteries by reductive leaching and solvent extraction with Cyanex 272, Hydrometallurgy 100 (2010) 168–171, https://doi.org/10.1016/j.hydromet.2009.10.010.

[12] L. Li, J. Lu, Y. Ren, X.X. Zhang, R.J. Chen, F. Wu, K. Amine, Ascorbic-acid-assisted recovery of cobalt and lithium from spent Li-ion batteries, J. Power Sour. 218 (2012) 21–27, https://doi.org/10.1016/j.jpowsour.2012.06.068.

[13] L. Sun, K. Qiu, Organic oxalate as leachant and precipitant for the recovery of valuable metals from spent lithium-ion batteries, Waste Manag. 32 (2012) 1575–1582, https://doi.org/10.1016/j.wasman.2012.03.027.

[14] C.L. Brierley, Biohydrometallurgical prospects, Hydrometallurgy 104 (2010) 324–328, https://doi.org/10.1016/j.hydromet.2010.03.021.

[15] Z. Chen, S. Wang, W. Liu, X. Gao, D. Gao, M. Wang, S. Wang, Morphology-dependent performance of Co_3O_4 via facile and controllable synthesis for methane combustion, Appl. Catal. A Gen. 525 (2016) 94–102, https://doi.org/10.1016/j.apcata.2016.07.009.

[16] W. Ahmad, T. Noor, M. Zeeshan, Effect of synthesis route on catalytic properties and performance of Co_3O_4/TiO_2 for carbon monoxide and hydrocarbon oxidation under real engine operating conditions, Catal. Commun. 89 (2017) 19–24, https://doi.org/10.1016/j.catcom.2016.10.012.

[17] G. Salek, P. Alphonse, P. Dufour, S. Guillemet-Fritsch, C. Tenailleau, Low-temperature carbon monoxide and propane total oxidation by nanocrystalline cobalt oxides, Appl. Catal. B 147 (2014) 1–7, https://doi.org/10.1016/j.apcatb.2013.08.015.

[18] T. Garcia, S. Agouram, J.F. Sánchez-Royo, R. Murillo, a.M. Mastral, A. Aranda, I. Vázquez, A. Dejoz, B. Solsona, Deep oxidation of volatile organic compounds using ordered cobalt oxides prepared by a nanocasting route, Appl. Catal. A Gen. 386 (2010) 16–27, https://doi.org/10.1016/j.apcata.2010.07.018.

[19] Z. Boukha, J. González-Prior, B. de Rivas, J.R. González-Velasco, R. López-Fonseca, J.I. Gutiérrez-Ortiz, Synthesis, characterisation and behaviour of Co/hydroxyapatite catalysts in the oxidation of 1,2-dichloroethane, Appl. Catal. B 190 (2016) 125–136, https://doi.org/10.1016/j.apcatb.2016.03.005.

[20] X. Xu, H. Han, J. Liu, W. Liu, W. Li, X. Wang, Promotional effects of samarium on Co_3O_4 spinel for CO and CH_4 oxidation, J. Rare Earths 32 (2014) 159–169, https://doi.org/10.1016/S1002-0721(14)60046-6.

[21] B. De Rivas, R. López-Fonseca, C. Jiménez-González, J.I. Gutiérrez-Ortiz, Synthesis, characterisation and catalytic performance of nanocrystalline Co_3O_4 for gas-phase chlorinated VOC abatement, J. Catal. 281 (2011) 88–97, https://doi.org/10.1016/j.jcat.2011.04.005.

[22] Z. Ren, Z. Wu, W. Song, W. Xiao, Y. Guo, J. Ding, S.L. Suib, P.-X. Gao, Low temperature propane oxidation over Co_3O_4 based nano-array catalysts: Ni dopant effect, reaction mechanism and structural stability, Appl. Catal. B 180 (2016) 150–160, https://doi.org/10.1016/j.apcatb.2015.04.021.

[23] A. Osman, J. Abu-Dahrieh, F. Laffir, T. Curtin, J. Thompson, D. Rooney, A bimetallic catalyst on a dual component support for low temperature total methane oxidation, Appl. Catal. B Environ. 187 (2016) 408–418.

[24] A.I. Osman, N. Ha, J. Abu-Dahrieha, F. Laffir, M. McLaren, M. Arredondo, J. Thompson, D. Rooney, An exceptionally active and stable catalyst for low temperature total methane oxidation, Appl. Catal. B Environ. 212 (2017) 68–79.

[25] M.V. Gallegos, L.R. Falco, M.A. Peluso, J.E. Sambeth, H.J. Thomas, Recovery of manganese oxides from spent alkaline and zinc-carbon batteries. An application as catalysts for VOCs elimination, Waste Manag. 33 (2013) 1483–1490, https://doi.org/10.1016/j.wasman.2013.03.006.

[26] L.R. Falco, A. Martinez, M. Di Nanno, H. Thomas, G. Curutchet, Study of a pilot plant for the recovery of metals from spent alkaline and zin-carbon batteries with biological sulphuric acid and polythionate production, Lat. Am. Appl. Res. 44 (2014) 123–129.

[27] Y.J. Liu, Q.Y. Hu, X.H. Li, Z.X. Wang, H.J. Guo, Recycle and synthesis of $LiCoO_2$ from incisors bound of Li-ion batteries, Trans. Nonferrous Met. Soc. China (English Ed.) 16 (2006) 956–959, https://doi.org/10.1016/S1003-6326(06)60359-2.

[28] Q. Meng, Y. Zhang, P. Dong, Use of glucose as reductant to recover Co from spent lithium ions batteries, Waste Manag. 64 (2017) 214–218, https://doi.org/10.1016/j.wasman.2017.03.017.

[29] X. Zhang, H. Cao, Y. Xie, P. Ning, H. An, H. You, F. Nawaz, A closed-loop process for recycling $LiNi_{1/3}Co_{1/3}Mn_{1/3}O_2$ from the cathode scraps of lithium-ion batteries: process optimization and kinetics analysis, Sep. Purif. Technol. 150 (2015) 186–195, https://doi.org/10.1016/j.seppur.2015.07.003.

[30] P. Meshram, B.D. Pandey, T.R. Mankhand, Hydrometallurgical processing of spent lithium ion batteries (LIBs) in the presence of a reducing agent with emphasis on kinetics of leaching, Chem. Eng. J. 281 (2015) 418–427, https://doi.org/10.1016/j.cej.2015.06.071.

[31] B. Faure, P. Alphonse, Co–Mn-oxide spinel catalysts for CO and propane oxidation at mild temperature, Appl. Catal. B 180 (2016) 715–725, https://doi.org/10.1016/j.apcatb.2015.07.019.

[32] S. Liu, Z. Wang, H. Zhao, T. Fei, T. Zhang, Ordered mesoporous Co_3O_4 for high-performance toluene sensing, Sens. Actuators B Chem. 197 (2014) 342–349, https://doi.org/10.1016/j.snb.2014.03.007.

[33] Z.Y. Tian, P.H. Tchoua Ngamou, V. Vannier, K. Kohse-Höinghaus, N. Bahlawane, Catalytic oxidation of VOCs over mixed Co-Mn oxides, Appl. Catal. B 117–118 (2012) 125–134, https://doi.org/10.1016/j.apcatb.2012.01.013.

[34] L. Xue, C. Zhang, H. He, Y. Teraoka, Catalytic decomposition of N_2O over CeO_2 promoted Co_3O_4 spinel catalyst, Appl. Catal. B 75 (2007) 167–174, https://doi.org/10.1016/j.apcatb.2007.04.013.

[35] S. Todorova, H. Kolev, J.P. Holgado, G. Kadinov, C. Bonev, R. Pereñíguez, A.C. Caballero, Complete n-hexane oxidation over supported Mn–Co catalysts, Appl. Catal. B 94 (2010) 46–54, https://doi.org/10.1016/j.apcatb.2009.10.019.

[36] S. Deng, N. Chen, D. Deng, Y. Li, X. Xing, Y. Wang, Meso- and macroporous coral-like Co_3O_4 for VOCs gas sensor, Ceram. Int. 41 (2015) 11004–11012, https://doi.org/10.1016/j.ceramint.2015.05.045.

[37] N. Zhang, Q. Qin, X. Ma, J. Zhou, L. Sun, C. Chen, S. Wen, Y. Chen, S. Ruan, One-step synthesis and gas sensing properties of hierarchical Fe doped Co_3O_4 nanostructures, J. Alloys. Compd. 723 (2017) 779–786, https://doi.org/10.1016/j.jallcom.2017.06.301.

[38] M. Konsolakis, S.A.C. Carabineiro, G.E. Marnellos, M.F. Asad, O.S. Soares, M.F.R. Pereira, J.J.M. Órfão, J.L. Figueiredo, Effect of cobalt loading on the solid state properties and ethyl acetate oxidation performance of cobalt-cerium mixed oxides, J. Colloid Interface Sci. 496 (2017) 141–149, https://doi.org/10.1016/j.jcis.2017.02.014.

[39] M. Piumetti, D. Fino, N. Russo, Mesoporous manganese oxides prepared by solution combustion synthesis as catalysts for the total oxidation of VOCs, Appl. Catal. B Environ. 163 (2015) 277–287, https://doi.org/10.1016/j.apcatb.2014.08.012.

[40] Y. Liu, H. Dai, J. Deng, S. Xie, H. Yang, W. Tan, W. Han, Y. Jiang, G. Guo, Mesoporous Co_3O_4-supported gold nanocatalysts: Highly active for the oxidation of carbon monoxide, benzene, toluene, and o-xylene, J. Catal. 309 (2014) 408–418, https://doi.org/10.1016/j.jcat.2013.10.019.

[41] R. Dedryvère, H. Martinez, S. Leroy, D. Lemordant, F. Bonhomme, P. Biensan, D. Gonbeau, Surface film formation on electrodes in a $LiCoO_2$/graphite cell: a step by step XPS study, J. Power Sour. 174 (2007) 462–468, https://doi.org/10.1016/j.jpowsour.2007.06.033.

[42] M.H. Castaño, R. Molina, S. Moreno, Cooperative effect of the Co–Mn mixed oxides for the catalytic oxidation of VOCs: Influence of the synthesis method, Appl. Catal. A Gen. 492 (2015) 48–59, https://doi.org/10.1016/j.apcata.2014.12.009.

[43] A. Rokicińska, M. Drozdek, B. Dudek, B. Gil, P. Michorczyk, D. Brouri, S. Dzwigaj, P. Kuśtrowski, Cobalt-containing BEA zeolite for catalytic combustion of toluene, Appl. Catal. B 212 (2017) 59–67, https://doi.org/10.1016/j.apcatb.2017.04.067.

[44] V.R. Mate, A. Jha, U.D. Joshi, K.R. Patil, M. Shirai, C.V. Rode, Effect of preparation parameters on characterization and activity of Co_3O_4 catalyst in liquid phase oxidation of lignin model substrates, Appl. Catal. A Gen. 487 (2014) 130–138, https://doi.org/10.1016/j.apcata.2014.08.023.

[45] D. Dobber, D. Döbber, D. Kießling, W. Schmitz, G. Wendt, MnO_x/ZrO_2 catalysts for the total oxidation of methane and chloromethane, Appl. Catal. B 52 (2004) 135–143, https://doi.org/10.1016/j.apcatb.2004.02.012.

[46] E. Zhecheva, R. Stoyanova, G. Tyuliev, K. Tenchev, M. Mladenov, S. Vassilev, Surface interaction of $LiNi_{0.8}Co_{0.2}O_2$ cathodes with MgO, Solid State Sci. 5 (2003) 711–720, https://doi.org/10.1016/S1293-2558(03)00096-7.

[47] K. Jirátová, J. Mikulová, J. Klempa, T. Grygar, Z. Bastl, F. Kovanda, Modification of Co-Mn-Al mixed oxide with potassium and its effect on deep oxidation of VOC, Appl. Catal. A Gen. 361 (2009) 106–116.

[48] J. Trawczynski, B. Bielak, W. Mista, Oxidation of ethanol over supported manganese catalysts—effect of the carrier, Appl. Catal. B: Environ. 55 (2005) 277–285.

[49] R. Wang, J. Li, Precursor and Sulfation on OMS-2 Catalyst for Oxidation of Ethanol and Acetaldehyde at Low Temperatures, Sci. Technol. 44 (2010) 4282–4287.

[50] M.V. Gallegos, M.A. Peluso, E. Finocchio, H.J. Thomas, G. Busca, J.E. Sambeth, Removal of VOCs by catalytic process, A study of MnZnO composites synthesized from waste alkaline and Zn/C batteries, Chem. Eng. J. 313 (2017) 1099–1111, https://doi.org/10.1016/j.cej.2016.11.001.

[51] M. Kamal, S. Razzak, M. Hossain, Catalytic oxidation of volatile organic compounds (VOCs) - A review, Atmosph. Env. 140 (2016) 117–134, https://doi.org/10.1016/j.atmosenv.2016.05.031.

[52] L.F. Liotta, M. Ousmane, G. Di Carlo, G. Pantaleo, G. Deganello, A. Boreave, A. Giroir-Fendler, Catalytic removal of toluene over Co_3O_4–CeO_2 mixed oxide catalysts: comparison with Pt/Al_2O_3, Catal. Lett. 127 (2009) 270–276, https://doi.org/10.1007/s10562-008-9640-0.

[53] V.P. Santos, S.A.C. Carabineiro, P.B. Tavares, M.F.R. Pereira, J.J.M. Órfão, J.L. Figueiredo, Oxidation of CO, ethanol and toluene over TiO_2 supported noble metal catalysts, Appl. Catal. B Environ. 99 (2010) 198–205, https://doi.org/10.1016/j.apcatb.2010.06.020.